Journal of Kerbala University , Vol. 7 No.1 Scientific. 2009

A Suggested Numerical Solution for the Master Equation of Nuclear Reaction

Dr. Mahdi Hadi Jasim[(1)], Dr. Shafik Shaker Shafik[(2)], and Ahmed Abdul-Razzaq Selman[(3)]
Department of Physics, College of Science, University of Baghdad, Baghdad-Iraq
PACS: 21.10.Ma; 24.10.Pa; 24.60.-k
[(1)]mhjasim@uobnpg.com
[(2)]ssalmola@uobnpg.com
(3)ahmed@aaselman.com

Abstract :

Numerical solution for the master equation of the preequilibrium statistical model has been presented, assuming one-component Fermi gas model. This numerical method has been shown to give the same accuracy for the simple as well as the more advanced schemes. The present method showed fast convergence for a wide range of physical system parameters and it was applied for two reaction examples that include neutron and proton induced reactions with ^{54}Fe nucleus at energies 20 and 80 MeV. Comparisons with standard earlier results indicated that the present method is proper for low reaction energies, but with worse accuracy at higher energies. The behavior of the present method was examined against the energy, exciton numbers, and time variation.

الخلاصة :

في البحث الحالي نقترح طريقة عددية لحل المعادلة الأساسية لأنموذج التفاعلات النووية الإحصائي بافتراض أن النواة تتألف من غاز فيرمي متكون من نوع واحد من الجسيمات. باستخدام الطريقة الحالية وجدنا أن دقة النتائج مقبولة عند استخدام أنموذج حسابي بسيط وكذلك نفس الدقة قد وجدت عند تطبيق نموذج أكثر تعقيدا، مما يدل على كفاءة الطريقة المقترحة. أثبتت الطريقة الحالية أنها متقاربة (convergent) لمدى واسع من مواصفات النظام المدروس. تم تطبيق هذه الطريقة على مثالين للتفاعلات النووية المحرضة بواسطة النيوترون والبروتون (nucleon induced reactions) مع نواة الحديد ^{54}Fe لطاقات 20 و 80 مليون إلكترون فولت. قورنت النتائج الحالية مع الطرق المعتمدة وتم التوصل إلى أن الطريقة الحالية تجمع كلا الدقة والبساطة مما يجعلها طريقة ملائمة للتطبيق في الحسابات العملية. بينت النتائج الحالية أن هذه الطريقة تمتاز بدقة مناسبة للأغراض الحسابية في الطاقات الواطئة، لكن الدقة تسوء عند الطاقات العالية. تم اختبار تصرف الطريقة الحالية مع الطاقة، عدد الجسيمات المؤقتة والزمن.

1. Introduction :

The preequilibrium statistical models are a group of models that are based on statistical approach to describe the various nuclear reactions at intermediate energies. This group include exciton model [1], Hybrid Model (HM) and Geometry Dependent Hybrid (GDH) model [2,3,4] and the Monte Carlo Hybrid (MCH) model [5,6]. These models have been developed rapidly since Griffin [1] put the exciton model as a semiclassical theory to explain the precompound nuclear emission (PE). The family of Hybrid models [2-6] are assumed as an improved version of Griffin's model where the basic ideas were combined with the Master Equation Model (MEM) due to Harp, Miller and Berne [7,8]. These models deal with the intermediate states of the nuclear reactions.The excitation development, when based on the residual two-body interaction, will ensure that the number of excitons characterizing each stage in the equilibration process will change by ±2 or zero. Equilibration process will cause creation of particle-hole pairs, and these pairs will be the reason that carries out the basic mechanism of energy share between the constituents of the nucleus, which leads to successive creation of excitons. Thus, each stage in the equilibration process can be specified by the exciton number n and excitation energy E. Decay may take place from these stages by a certain probability □, depending on n and E. The transition between adjacent stages is characterized by the transition rate, $\square_{x\text{-}y}$, between stages x and y as (Fermi golden rule),

$$\lambda_{x-y} = \frac{2\pi}{\hbar} M^2_{x-y}\, \omega_y \qquad (1),$$

where (*x*-*y*) represents (initial – final) destination, ω_y is the final accessible density of states. M_{x-y} is the matrix element of the specific interaction, $M_{x-y} = < y | \hat{M} | x >$, with $\hat{M}$ being the operator of the effective potential causing the system transition from (*x*) initial state to (*y*) final state. This important quantity, M_{x-y} is used by approximate formulae that are based on data extracted from experimental data [9]. Each stage has two transition possibilities, up and down, which means that the change of the exciton number $\Delta n = \pm 2$ or +2, and the inter-substages has $\Delta n = 0$. There is also a transition probability to the continuum which represents the decay of each stage.

The Master Equation (ME) describes the occupation probabilities for each stage. The ME will be given as, and in terms of one-component Fermi system [9],

$$\frac{dP(n,E,t)}{dt} = \lambda^{-}_{n+2}(n,E)\, P(n+2,E,t) + \lambda^{+}_{n-2}(n,E)\, P(n-2,E,t) - \frac{P(n,E,t)}{\tau_n(n,E)} \qquad (2),$$

where $P(n,E,t)$ is the occupation probability of the n^{th} stage with excitation energy E at time t, and $\lambda^{\pm}$ are the transition rates (in sec^{-1}) between two successive exciton states with $\Delta n = +2/-2$, and τ_n is the mean lifetime of this stage, defined as,

$$\tau_n(n,E) = \left(\lambda^{-}_n(n,E) + \lambda^{+}_n(n,E) + W(n,E)\right)^{-1} \qquad (3),$$

and $W(n,E)$ is the rate of decay to the continuum. Eq.(2) is the simple version of the two-component ME,

$$\begin{aligned}
\frac{dP(N,h_\pi,t)}{dt} = {} & \\
& \left[\lambda^{++}_{\nu\pi}(E,N-1,h_\pi) + \lambda^{++}_{\pi\pi}(E,N-1,h_\pi)\right] P(N-1,h_\pi-1,t) \\
& + \left[\lambda^{+0}_{\pi\nu}(E,N-1,h_\pi) + \lambda^{+0}_{\nu\nu}(E,N-1,h_\pi)\right] P(N-1,h_\pi,t) \\
& + \left[\lambda^{-0}_{\nu\nu}(E,N+1,h_\pi) + \lambda^{-0}_{\pi\nu}(E,N+1,h_\pi)\right] P(N+1,h_\pi,t) \\
& + \left[\lambda^{--}_{\pi\pi}(E,N+1,h_\pi+1) + \lambda^{--}_{\pi\nu}(E,N+1,h_\pi+1)\right] P(N+1,h_\pi+1,t) \\
& + \left[\lambda^{0+}_{\nu\pi}(E,N,h_\pi-1)\right] P(N,h_\pi-1,t) \\
& + \left[\lambda^{0-}_{\pi\nu}(E,N,h_\pi+1)\right] P(N,h_\pi+1,t) \\
& - \left[\lambda^{+0}_{\pi\nu}(E,N,h_\pi) + \lambda^{+0}_{\nu\nu}(E,N,h_\pi) + \lambda^{++}_{\nu\pi}(E,N,h_\pi) + \lambda^{++}_{\pi\pi}(E,N,h_\pi)\right. \\
& + \lambda^{-0}_{\nu\nu}(E,N,h_\pi) + \lambda^{-0}_{\pi\nu}(E,N,h_\pi) + \lambda^{--}_{\pi\pi}(E,N,h_\pi) + \lambda^{--}_{\pi\nu}(E,N,h_\pi) \\
& \left. + \lambda^{0+}_{\nu\pi}(E,N,h_\pi) + \lambda^{0-}_{\pi\nu}(E,N,h_\pi) + W(E,N,h_\pi)\right] P(N,h_\pi,t) \qquad (4),
\end{aligned}$$

where n_π and n_ν are the exciton numbers for protons and neutrons, respectively, they are related to n as $n = n_\pi + n_\nu$, and the occupation probability, $P(N, h_\pi, t)$, of n_π and n_ν number of excitons at time t and of excitation energy E. N is a function of n_π and n_ν number as: $n = p_\pi + h_\pi + p_\nu + h_\nu = 2(N+1) + n_o$, and n_o is the initial exciton number. h and p represent hole and particle numbers, and the subscripts π and ν represent proton and neutron types, respectively.

In this paper we shall use eq.(2) to explain the numerical procedure rather than eq.(4). Hopefully, the method applied here for one-component ME can be extended in the future for the more complicated two-component system.

The total lifetime for each of the states described by eq.(2) is given as [9],

$$T(n,E)=\int_0^{\infty} P(n,E,t)dt \qquad (5),$$

and if we assume that the emission will occur for a particle of type □ then the spectrum expected will be given by the following,

$$\frac{d\sigma_\beta(\varepsilon_\beta)}{d\varepsilon_\beta}=\sigma_\alpha \sum_{n_\pi,n_\nu} T(n,E)\,\lambda_\beta^c(\varepsilon_\beta;n,E) \qquad (6),$$

where □□ is the formation cross-section of the composite nucleus in the exit channel □□□the inverse cross-section). The decay rate □^{c}□ represents the partial emission rate of the particle □ from the state described by *n* and *E* into the final channel.

2. Earlier Methods of Solutions for the Master Equation

There are many suggested methods to find the solutions of the master equation, although the mathematical form seen from eq.(2) might appear simple. The difficulty in the ME is that each stage depends dynamically on the adjacent stages at the same time, *t*. The most important and popular methods are reviewed below.

Luider [10], assuming one-component Fermi system, showed that the ME can be given in the matrix form as,

$$[\dot{x}]=[A][x] \qquad (7),$$

where [*A*] is the matrix representing the decay rates,

$$[A]=\begin{bmatrix} \lambda_1^+ & -1/\tau_1 & \lambda_1^- & 0 & 0 & \dots & 0 & 0 \\ 0 & \lambda_2^+ & -1/\tau_2 & \lambda_2^- & & & & 0 \\ & & & & & & & \cdot \\ 0 & 0 & \dots & \dots & & & & \cdot \\ & & & & & & & \cdot \\ 0 & 0 & 0 & \dots & \lambda_n^+ & -1/\tau_n & \lambda_n^- & \end{bmatrix} \qquad (8),$$

and the solution [***x***] can then be represented as,

$$[A][T]=[x(t)]-[x_o] \qquad (9),$$

which assumes that [*x*(t)]≠0 at $t=\infty$. The form of *T* in eq.(9) is gven by eq.(5).

Dobeš and Běták [9] suggested further that the ME can be solved by iterative method for both one- and two-component systems, where eq,(2) is written as,

$$-D_n = x_{n-2}\,\tau_{n-2}\,\lambda_{n-2}^+ + x_{n+2}\,\tau_{n+2}\,\lambda_{n+2}^- - x_n \qquad (10),$$

which is divergent as long as the term $\left(\tau_{n-2}\,\lambda_{n-2}^+ + \tau_{n+2}\,\lambda_{n+2}^-\right)<1$, where,

$$x_n=\frac{T_n}{\tau_n} \qquad (11)$$

D_n is the initial condition. The iteration in this method starts from the zeroth approximation formula given by,

$$-D_n = T_{n-2}^{[0]}\,\lambda_{n-2}^+ + T_n^{[0]}/\tau_n \qquad (12),$$

and for n_o, and *n* states we have,

$$\left.\begin{aligned} T_{n_o}^{[0]} &= \tau_{n_o}\,D_{n_o} \\ T_n^{[0]} &= \tau_n\left(D_n + T_{n-2}^{[0]}\,\lambda_{n-2}^+\right) \end{aligned}\right\} \qquad (13),$$

n_o is the initial exciton number.

In the explicit method of Akkermans [11], one can write eq.(2) as a matrix form and the matrix [A], in a tri-diagonal matrix. The solution in this method is,

$$[t]=[B]\,[C]\,[q_o] \qquad (14).$$

This can be expanded in terms of power series to give,

$$T_n=\tau_n\,h_n\sum_{\substack{j=n_o\\ \Delta j=2}}^{n}(q_o)_j\left(\prod_{\substack{i=j\\ \Delta i=2}}^{n-2}\lambda_i^{+}\;\tau_i\;h_i\right) \qquad (15).$$

where if $j=n$, then we put the expression within the □ to be equal to unity.

The method above was further modified by Chatterjee and Gupta [12] who used elimination method. Dobeš and Běták [13] suggested yet another modified iterative method for two-component system where the ME solves to the following,

$$\begin{aligned}T^{[j+1]}(n_\pi,n_\nu)=\tau(n_\pi,n_\nu)\Big\{&T^{[j]}(n_\pi+2,n_\nu)\,\lambda^{-}(n_\pi+2,n_\nu)\\&+T^{[j]}(n_\pi,n_\nu+2)\,\lambda^{-}(n_\pi,n_\nu+2)+T^{[j]}(n_\pi+2,n_\nu-2)\,\lambda^{0}_{\pi\nu}(n_\pi+2,n_\nu-2)\\&+T^{[j]}(n_\pi-2,n_\nu+2)\,\lambda^{0}_{\nu\pi}(n_\pi-2,n_\nu+2)+T^{[j]}(n_\pi-2,n_\nu)\,\lambda^{+}(n_\pi-2,n_\nu)\\&+T^{[j]}(n_\pi,n_\nu-2)\,\lambda^{+}(n_\pi,n_\nu-2)+D(n_\pi,n_\nu)\Big\}\end{aligned} \qquad (16).$$

The parameters suggested in [9] were used to find the transition rates, namely,

$$|M_{\pi\nu}|^2=\frac{K}{A\;N\;Z\;E} \qquad (17-a),$$

$$|M_{\nu\nu}|^2=\frac{K}{A\;N^2\;R\;E} \qquad (17-b),$$

$$|M_{\pi\pi}|^2=\frac{K}{A\;Z^2\;R\;E} \qquad (17-c),$$

where: K=fitting parameter, R=a numerical factor that accounts for different ways of interaction between like and unlike types of particles. Its value is ~3. Ref.[9] used R=2.89 for proper treatment. A, Z and N= Atomic mass number, atomic number and neutrons number of the nucleus, and E=excitation energy of the nucleus.

Other methods such as those due to Kalbach [14] and Herman et al. [15] use explicit treatments to find the solution of the ME for two-component system.

3. Description of the Present Iterative Method

In the present paper, we suggest another method that we try to combine the iterative methods of Dobeš and Běták [9,13] and Luider[10] and Akkermans[11] methods, in simple numerical method. Suppose we have the ME written in the form,

$$\frac{dP_n}{dt}=\lambda^{-}_{n+2}P_{n+2}+\lambda^{+}_{n-2}P_{n-2}-\frac{P_n}{\tau_n} \qquad (18),$$

which is the same as eq.(2) but we omitted the dependence on E and t for simplicity. Using the finite difference scheme for replacing the time derivative, and writing the equations from n=1 to the n^{th} scheme, after defining the following factors,

$$\left.\begin{aligned}a_{j,1}&=\Delta t\,\lambda^{-}_{n+2}\\ a_{j,2}&=\left(1-\frac{\Delta t}{\tau_n}\right)\\ a_{j,3}&=\Delta t\,\lambda^{+}_{n-2}\end{aligned}\right\} \qquad (19),$$

where the index j is related to n by the simple relation, $j = \frac{n+1}{2}$. Then, the ME simply solves to the following,

$$P_i^{n+1} = \sum_{k=1}^{3} a_{j,k} P_i^n \qquad (20).$$

This simple equation will converge with initial conditions,

$$\left.\begin{aligned} P_{i=0}^{n_o} &= 1 \\ P_{i=0}^{n} &= 0 \end{aligned}\right\} \qquad (21),$$

which is convergent as long as the factors a's are convergent. This simple method is actually based on Euler difference scheme. One may argue that this simple method is of less accuracy than the above mentioned methods, however, a practical comparison shows that the difference of the occupation probability between this method and the earlier method is less than ~ 5%. Combining this level of accuracy with the relatively simple programming effort, the method suggested in the present paper shows its importance. Beside this, the method can be easily improved to include any number of excitons, n. Other methods of difference schemes, such as Runge-Kutta method, was also examined numerically against the present method and the difference was also promising as will be seen in the next paragraph, where numerical calculations are described for selected examples and comparisons are presented to test this method.

It should be mentioned that, regardless its simplicity, the method suggested here should be carefully applied with suitable choice of the time step, Δt, just as in any ordinary differential equation when one seeks numerical solution. Convergence might never be reached if this parameter were of order of Δ_n or larger. However, the simplicity of this method suggests that one can try a set of values for Δt, and select the best (leading to a suitably convergent) solution.

4. Results, Discussion of Numerical Calculations, and Comparisons

The current method is given in general by eqs.(18–21). Two different numerical methods were used in order to find the time derivative of the occupation probability, namely, Euler (centered) method and Runge-Kutta method. In order to perform numerical calculations, the transition rates given in the ME are used assuming two approaches, the first is the experimentally evaluated transition rate (according to the most recent formulae due to Kalbach [17, 18]), namely,

$$|M|^2 = K \frac{A_\beta}{g_o^3} \left(\frac{E}{3A_\beta} + 20.9 \right)^{-3} \quad \text{(MeV)} \qquad (22),$$

where A_β is the mass number of the incident projectile, g_o is the single-particle state density, and K is a constant that has the value 900 MEV^2 for proton-proton and 2200 MeV^2 for neutron-neutron reaction. In this paper, we assumed that the excitation is mainly due to neutron-neutron and proton-proton reaction only, and we shall ignore neutron-proton one. The second approach is to assume that the transition rates are all equal in either ways, i.e., with Δn= +2 and -2, and are replaced by unity in order to obtain the relative occupation probabilities in each exciton configuration. These details will lead to four different applications of the method suggested in this paper. Furthermore, the entire set above was applied for four examples, namely, (n+^{54}Fe) and (p+^{54}Fe) reactions at nucleon incident energies 20 and 80 MeV. This verity of cases will ensure careful investigation of the results of this work with other references for practical comparison. All of the numerical examples described below are written in Matlab. The value of the single-particle density g_o was fixed at 14 MeV^{-1} in all calculations of the present paper. The occupation probabilities which represent the solution of the ME are given in percentage for the purpose of clear comparisons. Below are the applications of the suggested method.

4.1. Euler Scheme with Energy-Dependent Matrix Elements

The results are shown in Figs.(1-A and B), for neutron at incident energies 20 and 80 MeV, respectively, for exciton numbers 1, 3 and 5. From these figures, one immediately notices how the system changes with time, *t*, exciton number *n* and energy of the incident particle. The initial conditions imposed are according to Dobeš and Běták [9]. First, as the exciton number increases, one can see that the distribution peak shifts towards longer time. Due to these specific observations of the ME, it was suggested [2, 4] that there is a certain exciton number that is called "the most probable exciton number $\bar{n}$" from which nuclear reaction is most expected to terminate by forming the compound nucleus. In the examples above, only few exciton numbers were considered, *n*=1, 3 and 5. Although these exciton numbers are far less than $\bar{n}$, and still important because nuclear preequilibrium decay is most probable from these low exciton numbers [9,11,14-16]. An interesting observation is that at *n*=1 the occupation probability (hence the total lifetime *T*) of the system behaves ideally as the usual nuclear (exponential) decay law. This behavior, in fact, is a direct consequence of the initial condition imposed by the program, that is at t=0, P_1=1. Still, this result might indicate that there is a possibility to find analytical solution that depends exponentially on time and transition rates. This interesting point will be studied in the future. The analytical solutions presented in Section II due to Luider [10], Akkermans [11] and Dobeš and Běták [9] have quite level of complexity, so a simple analytical solution, if exist, will highly simplify the problem of PE calculations. Also, from Figs.(1-A and B), the effect of energy on the total behavior is quite obvious. As the energy increases from 20 to 80 MeV, the system reaches faster to balanced (equilibrated) state even at these low exciton numbers. Energy effect can be seen to effect the entire behavior where: (*a*) the probabilities decay faster to equilibrated states, (*b*) the centers corresponding to the maxima happen at shorter lifetime, and (*c*) the tail of all the curves becomes more dependent on *t*. Figs.(1-C and D) represent the calculations made for ($p+^{54}Fe$) reaction. Again, the effect of energy is seen for comparing these figures with each others on one side, and with those of Figs.(1-A and B) on the other hand. From the second comparison, one understands how different the behavior of the system will be when the incident particle comes with unit charge. These effects are, in fact, extremely dominate at nuclear reactions at low energies as seen from Figs.(1-A and C). From Figs.(1-C and D), the same effect is seen for energy change for the same type of incident particle. In these examples, the system tends to be equilibrated even faster that in the case for neutron reaction. Such results, which indicate the rapid energy share between the incident particle and the nucleus, show that proton reactions have, in general, more details that should be taken into account when investigating any of the statistical models applications for nuclear reactions.

4.2. Euler Scheme with Energy-Independent Matrix Elements

The results of these calculations are shown in Figs.(2-A and B). In this case, proton and neutron reactions will read the same as seen from eq.(22). Thus, the major difference will be due to energy change of the incident particle, not the *type* of the particle itself. Of course, energy-independent matrix element is considered as a crude approximation in the physics of nuclear reaction. This case, therefore, seems to be not precise in practical calculation; nevertheless, it can be used for the present comparison for clarity of the method suggested herein. These figures show that the probabilities become less dependent on *t* if the matrix elements were energy-independent. The spread of the curves in the case of 20 MeV is even wider than that of Fig.(1-A). This signifies the importance of energy dependence for various cases that needed to be taken under investigation during compound nucleus formation. A glance on these figures indicates that as the incident energy increases the occupation probabilities fall faster with time. In At energy 20 MeV the occupation probability is less dependent on *t*, and at energy 80 MeV, these probabilities are more dependent on *t*. This means that in this approximation the method adopted in this paper might fail to reproduce the same accuracy when <u>*not*</u> dealing with the more realistic energy-dependent matrix element during calculating the transition rates. So this point adds another restriction on the present method.

However, most sensible PE calculations deal with the realistic case, i.e., that these matrix elements depend on *E* in one way or another. Therefore, the numerical method presented here is still of meaning to be considered in the cross-section calculations.

4.3. Runge-Kutta Method with Energy-Dependent Matrix Elements

The same examples above were applied using Runge-Kutta method in order to test the accuracy of the present method. Runge-Kutta method is of high accuracy than the simple Euler method and, as one may expect, Runge-Kutta method needs much more complicated numerical scheme and programming effort. The results of comparison of the two method against each other is presented in Figs.(3-A and B). This example is intended to be compared with the results of Figs.(1-C and D), i.e., for ($p+^{54}Fe$) reaction at energies 20 and 80 MeV, respectively. Similar input parameters were used in all cases of Figs.(3-A and B). The consistency of the present method, eq.(21), is shown to be acceptable to an approximate degree at low energy, while at energy 80 MeV the difference is quite obvious. Therefore, it is emphasized that the simple numerical scheme proposed above *should* be applied at energies around 20 MeV. At higher energies, more complicated methods must be used. The results of the other examples were seen to have the same behavior for other examples as in Figs.(3-A and B), i.e., as the energy increased from 20 to 80 MeV, the difference between the two methods becomes more clear. Therefore, no other comparisons will be made here.

5. Conclusions

The important conclusions can be summarized as follows:

(a) The master equation can be solved numerically using simple version of Euler scheme, but can only be applied at low energies.

(b) Other complicated approaches such as Runge-Kutta method, or any of the numerical methods described earlier in Section II, is needed if the problem extends to high reaction energies.

(c) The occupation probabilities behave as slow functions of time at low energies, and tend to drop faster with more dependence on time at high energies.

(d) As the exciton number increases above unity, the peaks of the occupation probabilities are shifted toward longer lifetimes, whereas at n=1 the occupation probability behaves almost in exponentially decreasing manner.

(e) At large exciton number the dependence of the occupation probability on time and energy becomes insignificant which suggests that there is a maximum exciton number possible to be accessed by the system before statistical and thermal nuclear equilibrium.

Reference:

[1] J. J. Griffin, "*Statistical Model of Intermediate Structure*", *Phys. Rev. Lett.*, 17(1966)478, also see M. Blann, "*Preequilibrium Decay*," *Ann. Rev. Nucl. Sci*. 25(1975)123;

[2] M. Blann, "*Extension of Griffin's model for medium-energy nuclear reactions*," *Phys. Rev. Lett.* 18(1968)1357.

[3] M. Blann, "*Hybrid Mode for Pre-Equilibrium Decay in Nuclear Reactions*", *Phys. Rev. Lett.* 27(1971)337.

[4] M. Blann, "*Importance of Nuclear Density Distribution on Pre-Equilibrium Decay" Phys. Rev. Lett.* 28(1972)757.

[5] M. Blann and M. B. Chadwick, "*New Precompound Decay Model: Angular Distributions*", *Phys. Rev.* C57(1998)233.

[6] M. Blann "*New Precompound Decay Model*", *Phys. Rev.* C57(1998)233.

[7] G. D. Harp, J. M. Miller and B. J. Berne, "*Attainment of Statistical Equilibrium in Excited Nuclei*", *Phys. Rev*. 165(1968)1166, and 165(1968)1174E.

[8] G. D. Harp and J. M. Miller, "*Precompound Decay from Time-Dependent Point of View*", *Phys. Rev*. C3(1971)1847.

[9] J. Dobeš and E. Běták, "*Fast and Precise Exciton Model Calculations of the Nuclear Reactions* ", *Z. Phys*. A288 (1978)175.
[10] F. J. Luider, "*Note on the Solution of the Master Equation in the Exciton Model of Preequilibrium Theory", Z. Phys*. A284 (1987)187.
[11] J. M. Akkermans, "*On the Calculation of Mean Lifetimes in the Preequilibrium Exciton Model*", *Z. Phys*. A292 (1979)57.
[12] S. K. Gupta, "*Two-Component Equilibration in the Exciton Model of Nuclear Reactions*", *Z. Phys*. A303 (1981)329, and A. Chatterjee and S. K. Gupta, "*Closed Expressions for Mean Lifetimes in the Exciton Model*", *Z. Phys*. A301 (1981)271.
[13] J. Dobeš and E. Běták, "*Two-Component Exciton Model*", *Z. Phys*. A310 (1983)329.
[14] C. Kalbach, "*Two-Component Exciton Model: Basic Formalism Away From Shell Closures." Phys. Rev*. C33(1986)818.
[15] M. Herman, G. Reffo, and C. Costa, "*Early Stage Equilibrium Dynamics in a Two-Component Nuclear System*", *Phys. Rev.* C39 (1989) 1269
[16] C. K. Cline and M. Blann, "*The Pre-Equilibrium Statistical Model: Description of the Nuclear Equilibration Process and Parameterization of the Model*", *Nucl. Phys*. A172(1971)225.
[17] C. Kalbach, "*Users Manual of PRECO-2006*" Brookhaven National Laboratory (July 2007):
[18] C. Kalbach, "*Missing Final States And The Spectral Endpoint In Exciton Model Calculations*", *Phys. Rev*. C73(2006)024614.

Figure Caption:

Fig.(1-A). The time-distribution of the occupation probabilities for n=1, 3 and 5, using Euler centered scheme for (n+^{54}Fe) reaction at incident energy 20 MeV.
Fig.(1-B). The same as Fig.(1-A) for incident energy 80 MeV.
Fig.(1-C). The same as Fig.(1-A) for (p+^{54}Fe) reaction at incident energy 20 MeV.
Fig.(1-D). The same as Fig.(1-C) at incident energy 80 MeV.
Fig.(2-A). The same as Fig.(1-A) for (p+^{54}Fe) reaction at incident energy 20 MeV.
Fig.(2-B). The same as Fig.(2-A) at incident energy 80 MeV.
Fig.(3-A). The solution of the ME for (p+^{54}Fe) reaction at incident energy 20 MeV using both Euler method (bold lines) and Runge-Kutta method (thin lines).
Fig.(3-B). The same as Fig. (3-A) for 80 MeV.

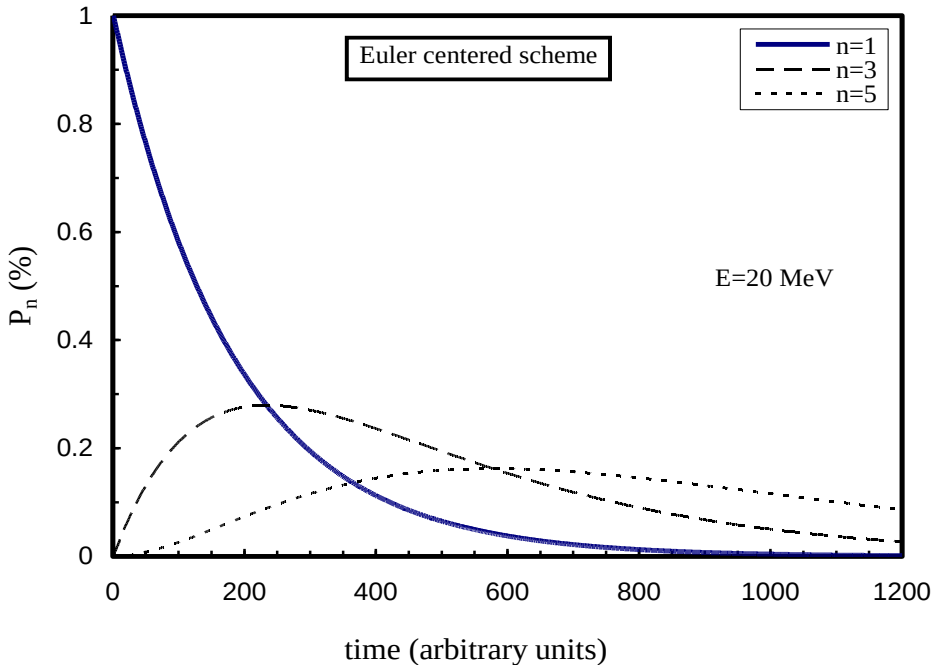
Euler centered scheme
n=1
n=3
n=5
E=20 MeV
P_n (%)
0
0.2
0.4
0.6
0.8
1
0
200
400
600
800
1000
1200
time (arbitrary units)

Fig(1-A)

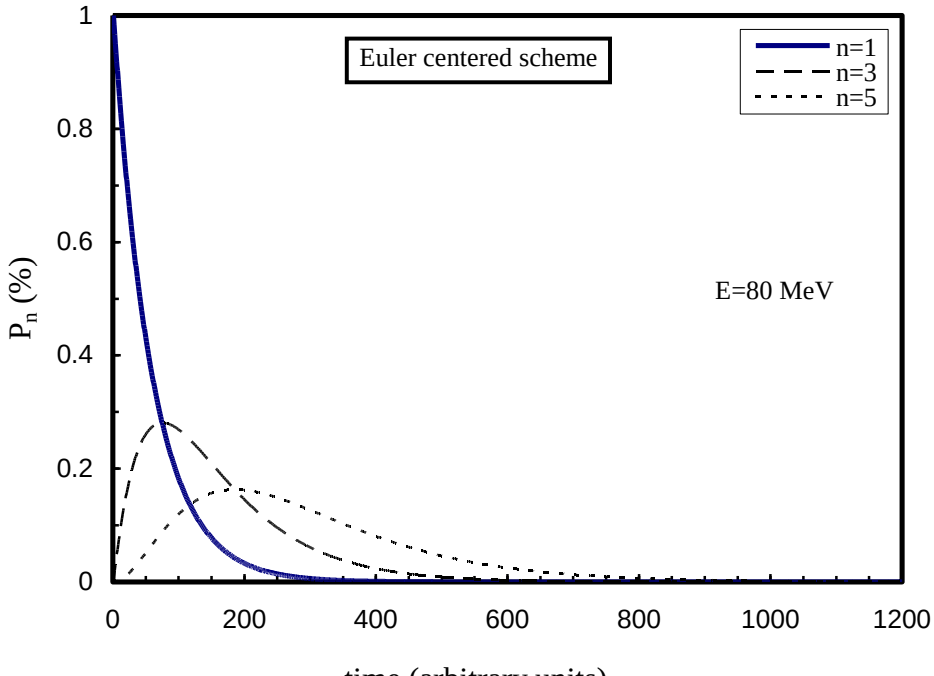
Euler centered scheme
n=1
n=3
n=5
E=80 MeV
P_n (%)
0
0.2
0.4
0.6
0.8
1
0
200
400
600
800
1000
1200
time (arbitrary units)

Fig(1-B)

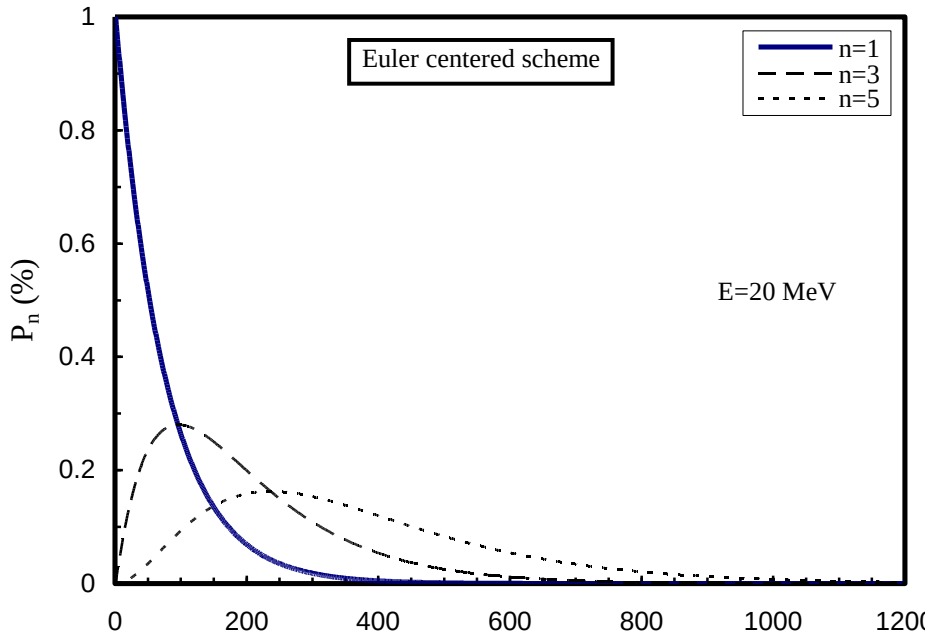
Euler centered scheme
n=1
n=3
n=5
E=20 MeV
P_n (%)
time (arbitrary units)

Fig(1-C)

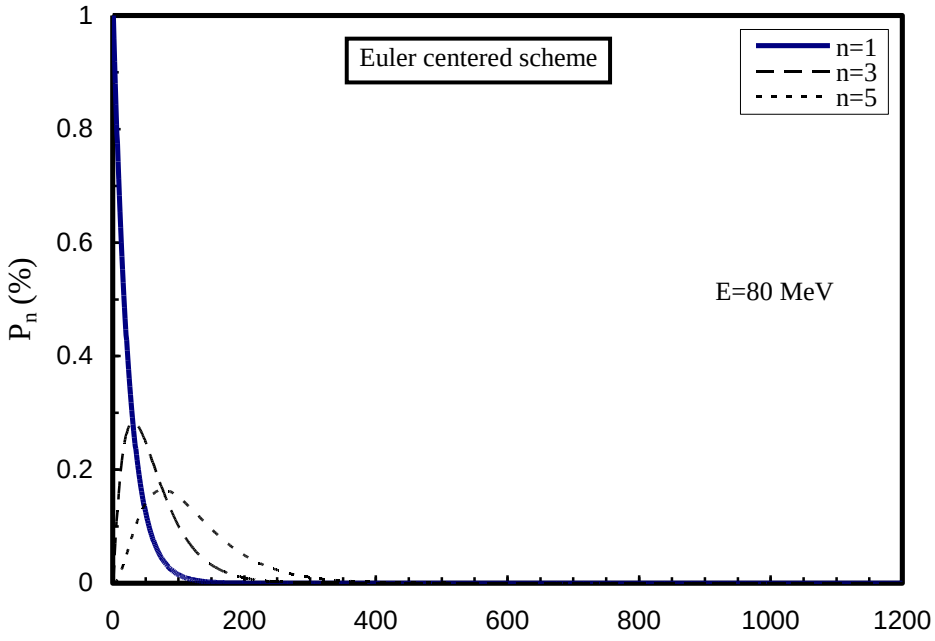
Euler centered scheme
n=1
n=3
n=5
E=80 MeV
P_n (%)
time (arbitrary units)

Fig(1-D)

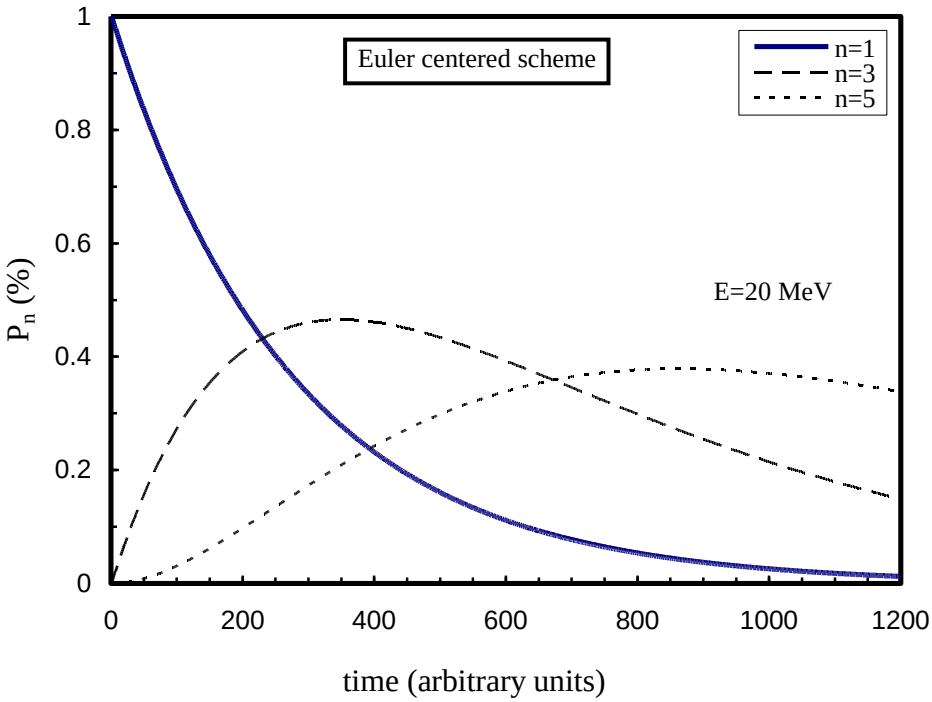
Euler centered scheme
n=1
n=3
n=5
E=20 MeV
P_n (%)
time (arbitrary units)

Fig(2-A)

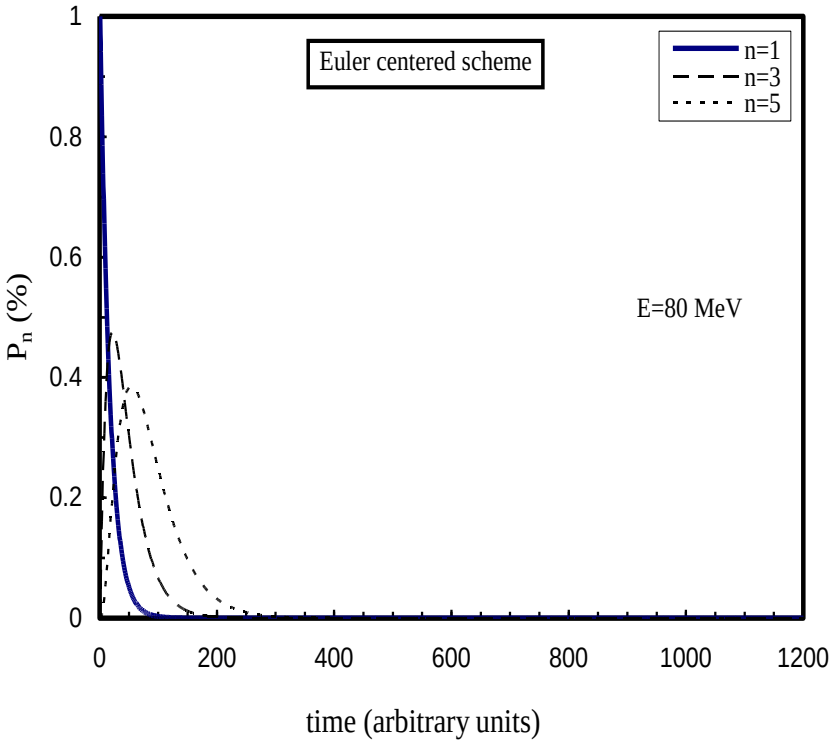
Euler centered scheme
n=1
n=3
n=5
E=80 MeV
P_n (%)
time (arbitrary units)

Fig(2-B)

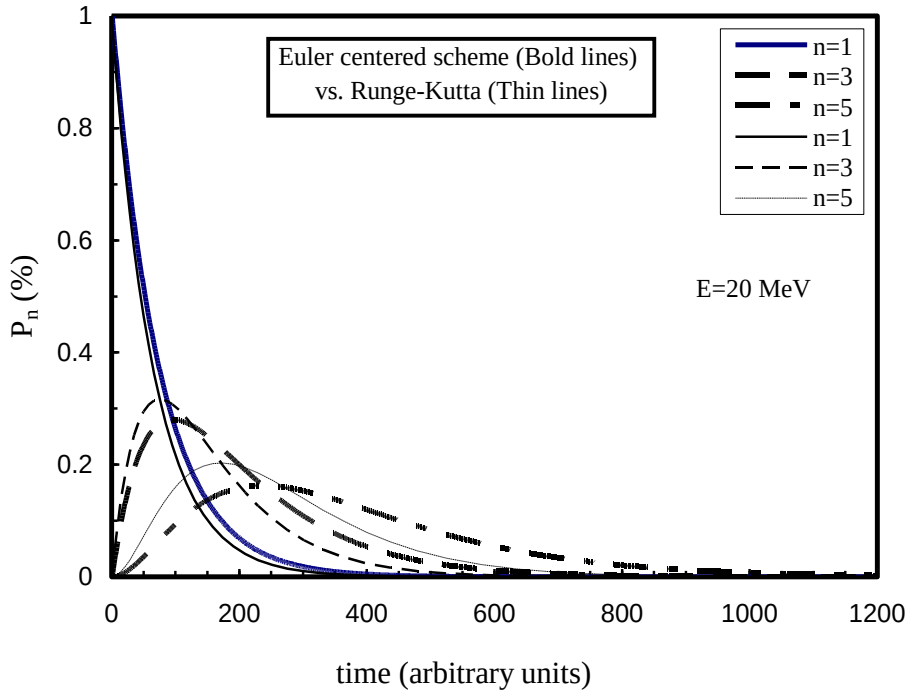
Euler centered scheme (Bold lines)
vs. Runge-Kutta (Thin lines)
n=1
n=3
n=5
n=1
n=3
n=5
E=20 MeV
P_n (%)
time (arbitrary units)

Fig(3-A)

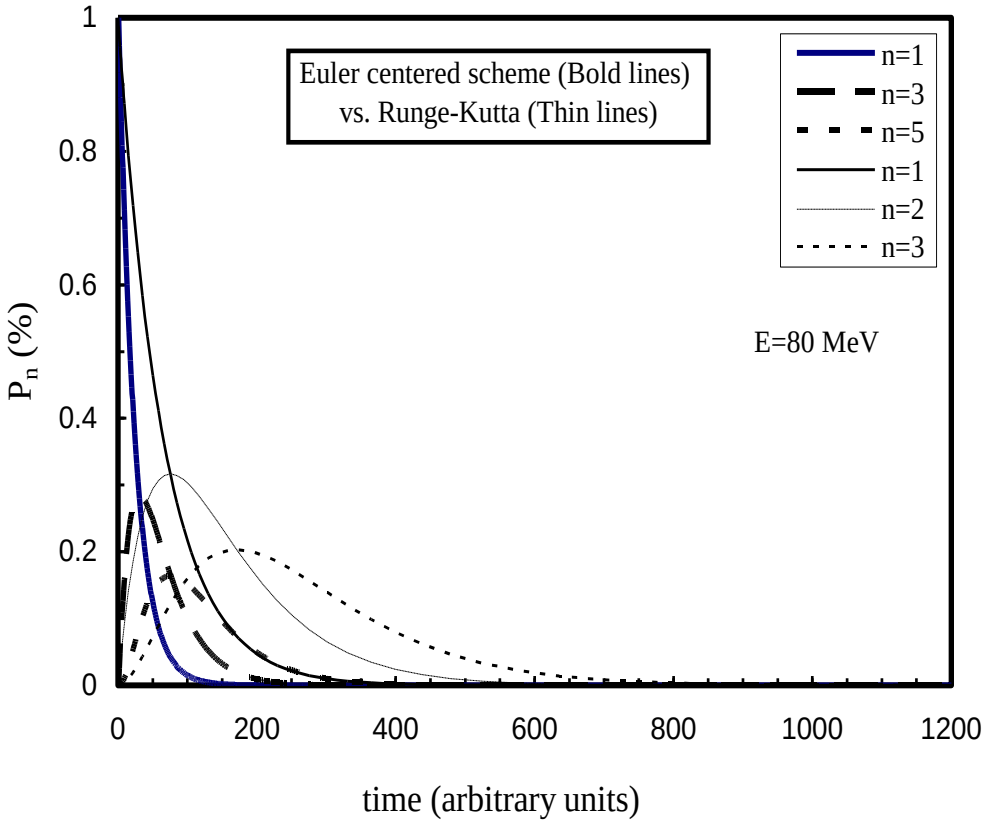
Euler centered scheme (Bold lines)
vs. Runge-Kutta (Thin lines)
n=1
n=3
n=5
n=1
n=2
n=3
E=80 MeV
P_n (%)
time (arbitrary units)

Fig(3-B)